

DOI: <https://doi.org/10.17816/fm7512>

Морфологическое исследование газобетонных блоков при ударном воздействии 9-миллиметрового снаряда под разными углами

М. Сингх¹, Р. Рохатги¹, С. Кумар², С. Гупта³¹ Национальный институт криминологии и судебной экспертизы, Нью-Дели, Индия;² Национальный университет судебных наук — Исследовательский центр баллистики и испытательный полигон, Гандинагар, Индия;³ Отделение судебной медицины и токсикологии Всеиндийского института медицинских наук, Раджкот (Гуджарат), Индия

АННОТАЦИЯ

Обоснование. Бетонные конструкции, используемые в защитных сооружениях, таких как склады боеприпасов и bunkеры, подвержены ракетным ударам, что требует проведения комплексной баллистической оценки, включающей механизмы проникания и перфорации. Большинство эмпирических и аналитических моделей проникания снарядов в бетон направлены, прежде всего, на определение глубины проникания, скалывания и толщины перфорации. В бетонных конструкциях, подвергшихся огневому воздействию, наблюдаются различные типы разрушений, которые могут с идентификацией использованного огнестрельного оружия и возможных огневых позиций.

Цель исследования — изучить особенности огневого воздействия на газобетонные блоки 9-миллиметрового снаряда в цельнометаллической оболочке, выпущенного с дистанции 5 м под разными углами. Задача состоит в том, чтобы сформировать гипотезы и выводы, основанные исключительно на наблюдаемых повреждениях, возникающих в результате попадания пули. Тщательный анализ полученных повреждений может дать много полезной информации.

Материалы и методы. В исследовании использованы 12 газобетонных блоков, в каждый из которых были выпущены пули калибра 9×19 мм под четырьмя различными углами (0°, 15°, 30°, 45°). Зависимость между углом встречи пули с преградой и размером входного отверстия определяли методом подгонки эллипса.

Результаты. Изучение картины разрушений показало, что при угле встречи 0° имелись значительные повреждения как на входном, так и выходном отверстиях. С увеличением угла встречи диаметр выходного отверстия постепенно уменьшался, и в итоге при угле 45° перфорация полностью отсутствовала. Эта тенденция коррелирует с характером разрушений вблизи входного и выходного отверстий, а также с рассеиванием энергии в точке удара, соответствующей углу встречи.

Заключение. Отмечена тенденция между потерей энергии снаряда при ударе и последующим повреждением поверхности газобетонных блоков. Анализ частиц газобетонного блока, оставшихся на пулях, а также деталей нарезки поможет в определении характеристик огнестрельных отверстий и огнестрельного оружия, обнаруженного на месте преступления.

Ключевые слова: криминалистическая баллистика; 9-миллиметровый снаряд; газобетонные блоки; траектория, перфорация.

Как цитировать:

М. Сингх, Р. Рохатги, С. Кумар, С. Гупта. Морфологическое исследование газобетонных блоков при ударном воздействии 9-миллиметрового снаряда под разными углами // *Судебная медицина*. 2023. Т. 9, № 3. С. 255–267. DOI: <https://doi.org/10.17816/fm7512>

DOI: <https://doi.org/10.17816/fm7512>

Morphological study of fly-ash block under angular impact of 9 mm projectile

Malika Singh¹, Richa Rohatgi¹, Saurabh Kumar², Sanjay Gupta³

¹ LNJN NICFS National Forensic Sciences University, New Delhi, India;

² National Forensic Sciences University – Ballistics Research Centre & Testing Range, Gandhinagar, India;

³ Department of Forensic Medicine & Toxicology, All India Institute of Medical Sciences, Rajkot (Gujarat), India

ABSTRACT

BACKGROUND: Concrete structures utilized in protective buildings such as ammunition depots and bunkers are susceptible to missile impacts, necessitating a comprehensive ballistic assessment involving penetration and perforation mechanics. Most of the empirical and analytical models for projectile penetration in concrete primarily focus on determining the penetration depth, scabbing, and perforation thicknesses. Concrete structures subjected to firearm attacks exhibit distinct fracture modes that can aid in identifying the firearm used and potential firing locations.

AIM: This study aims to comprehend the effects of the angular firing of a 9 mm full metal jacketed projectile on aerated concrete blocks, fired from a 5 m range. The goal is to generate hypotheses and conclusions based solely on the observable damage resulting from bullet impacts. A meticulous analysis of the incurred damages can unveil a range of possibilities.

MATERIALS AND METHODS: The sample comprised 12 aerated concrete blocks, each subject to 9×19 mm bullets fired from four different angles: 0°, 15°, 30°, and 45°. The relationship between impact angle and entry hole dimensions was established using the best-fit ellipse method.

RESULTS: Examination of the fracture pattern revealed significant damage at both entry and exit holes for a 0° impact angle. As the impact angle increased, the exit hole diameter progressively decreased, culminating in no perforation at a 45° angle. This trend correlated with fracture patterns near entry and exit holes, along with energy dissipation at the impact site corresponding to the impact angle.

CONCLUSION: A trend was observed between projectile energy loss upon impact and resultant damage to aerated concrete block surfaces. Analysis of aerated concrete block components deposited on the bullets, including rifling details, can help link them to the gunshot openings and firearms recovered at crime scenes.

Keywords: forensic ballistics; 9 mm projectile; fly ash; trajectory; perforation.

To cite this article:

Singh Malika, Rohatgi Richa, Kumar Saurabh, Gupta Sanjay. Morphological study of fly-ash block under angular impact of 9 mm projectile. *Russian Journal of Forensic Medicine*. 2023;9(3):255–267. DOI: <https://doi.org/10.17816/fm7512>

Received: 26.04.2023

Accepted: 02.08.2023

Published: 28.09.2023

DOI: <https://doi.org/10.17816/fm7512>

9mm弹丸角度冲击下的飞灰块形态研究

Malika Singh¹, Richa Rohatgi¹, Saurabh Kumar², Sanjay Gupta³

¹ LNJN NICFS National Forensic Sciences University, New Delhi, India;

² National Forensic Sciences University – Ballistics Research Centre & Testing Range, Gandhinagar, India;

³ Department of Forensic Medicine & Toxicology, All India Institute of Medical Sciences, Rajkot (Gujarat), India

简评

论证。弹药库和地堡等防护建筑中使用的混凝土结构很容易受到导弹的冲击，因此有必要进行涉及穿透和射孔力学的综合弹道评估。弹丸穿透混凝土的大多数经验和分析模型主要侧重于确定穿透深度、碎甲和射孔厚度。受到火器攻击的混凝土结构会表现出不同的断裂模式，这有助于确定所使用的火器和潜在的发射位置。

目的。本研究旨在了解从5m射程内发射的9mm全金属护套弹丸角度冲击对AAC块的影响。目的是仅根据子弹撞击造成的可观察到的损坏来提出假设和结论。对造成的损坏进行细致分析可以发掘一系列机会。

材料和方法。样品由12块AAC块组成，每块都受到从0°、15°、30°和45°四个不同角度发射的9×19mm子弹的打击。采用最佳拟合椭圆法确定了撞击角度与弹孔尺寸之间的关系。

结果。对断裂模式的检查发现了，在0°的冲击角下，入口和出口孔都有明显的损坏。随着冲击角度的增大，出口孔直径逐渐减小，最终在45°角下没有射孔。这一趋势与入口和出口孔附近的断裂模式相关以及与冲击角度相对应的冲击部位的能量耗散相关。

结论。观察到弹丸冲击时能量损失与AAC块表面受损之间的趋势。对沉积在子弹上的AAC块状部件（包括膛线细节）进行分析，有助于将它们与犯罪现场发现的枪眼和枪支联系起来。

关键词：法医弹道学鉴定；9mm的弹丸；飞灰；弹道；射孔。

引用本文：

Singh Malika, Rohatgi Richa, Kumar Saurabh, Gupta Sanjay. 9mm弹丸角度冲击下的飞灰块形态研究. *Russian Journal of Forensic Medicine*. 2023;9(3):255–267. DOI: <https://doi.org/10.17816/fm7512>

收到: 26.04.2023

接受: 02.08.2023

发布日期: 28.09.2023

BACKGROUND

Forensic investigators use different methods to establish the forensic significance of fired projectiles. These methods help them in conducting effective investigations to support legal proceedings. When a projectile hits a target, the outcomes are contingent on the encountered barriers. The effects of one or more interactions between a projectile and barriers that prohibit its penetration at potentially lethal velocities for vulnerable components constitute the terminal ballistics of a projectile. The primary goal of a barrier is to decelerate the projectile, achieved through fragmentation or deformation. The projectile's velocity is partially influenced by factors including propellant type, ignition, and subsequent high-pressure gas expansion that propels the projectile from the weapon's barrel at a substantial muzzle velocity [1, 2]. Understanding the mechanical behavior of solids is essential to establish a foundation for selecting barrier parameters crucial in defining terminal interactions [3]. Concrete, showing distinct characteristics under tension and compression, presents a more intricate challenge in ballistic assessment compared to metals. These characteristics help in identifying the firearm used and potential firing locations. Significant differences in the physical properties of metals, concrete, and masonry govern the resisting forces against penetration and the fracture mechanisms leading to perforation. Concrete structures under firearm attacks can experience diverse fracture modes, including complete fracture, penetration, perforation (full penetration), scabbing, spalling, cracking, local plugging, and/or global failure (as shown in Figure 1) [4]. Among these, perforation inflicts the most severe damage, while spalling and scabbing, accompanied by craters at entry and exit points, represent common failure modes [2].

The trajectory of a bullet holds crucial importance in reconstructing crime scenes, significantly impacting bullet performance. As a bullet exists the barrel, it follows a

parabolic trajectory, curving downward. Regardless of the muzzle velocity, the bullet experiences an approximate 1.15 m drop in half a second of flight. Point-blank range shots exhibit an almost flat trajectory. The angle of elevation, muzzle velocity, and bullet shape collectively determine the bullet's maximum attainable range. Reconstructing a crime scene based on bullet trajectory involves analyzing primary bullet defects, shape, dimensions, and the spatial relation among primary, secondary, and tertiary bullet defects [1, 5].

AIM

The reconstruction of firearm-involved crime scenes requires identifying fired-shot characteristics. This study aims to determine bullet trajectories, aiding in establishing the firing direction, location, suspect height, and firing angle. Through meticulous analysis of damages caused by a 9mm full metal jacketed projectile on AAC blocks at various angles, diverse possibilities were obtained. Therefore, this study spans different firing ranges for angles of 0°, 15°, 30°, and 45°. The objectives are to determine the shooter positions, establish a connection between energy loss and the damage caused by the 9 mm projectile on the AAC block with varying firing angles, and establish a relationship between the bullet trajectory and angles by considering the structural dimensions of entry and exit points.

MATERIALS AND METHODS

Sample Preparation and Projectile Selection

The study utilized AAC blocks manufactured in accordance with BIS Standard for Concrete Masonry Units Part 3 Autoclaved Cellular (Aerated) Concrete Blocks (IS 2185 Part-3:1984). AAC blocks are made by the formation of calcium silicate hydrate, achieved by reacting sand with calcium hydroxide under steam and pressure curing in an autoclave for 14 to 18 hours. These blocks, commonly employed in constructing walls for houses and bridges, were suitable for the study's objectives. The physical specifications of the AAC blocks are detailed in Table 1 [6, 7].

The firing of ammunition was executed using a 9 × 19 mm test barrel. A laser was attached to the top of the universal barrel to aid in pinpointing the impact location on the target. Standard 9 × 19 mm rimless, center fire type, ball cartridges (manufactured in 2015/ India) were used. The bullets were full metal jacketed round-nosed, featuring a lead-antimony core encased in gilding-metal (Table 2). The cartridges were tightly coned onto the bullets [8]. The muzzle velocity of the ammunition was measured using Intelligent IR Gate, with BMS Test Velocity LG software calculating velocities on a connected computer via Ethernet. Velocity was maintained at 430±15 m/s. Preliminary blank aiming was conducted, with reloading performed as needed to attain the desired velocity using a reloading unit. The characteristics of the 9 mm ball, both physical and performance-related, are outlined in Table 2.

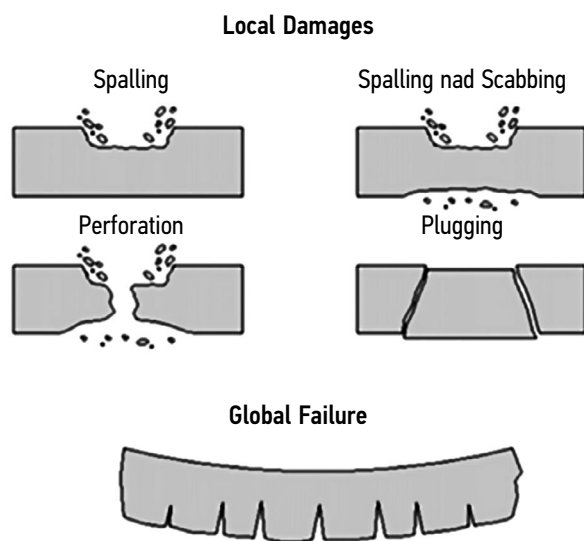


Fig. 1. Local Damages and Global Failure.

Table 1. Physical Specifications of AAC Block

Test Parameters (Physical Tests)	Specified Requirements As Per IS 2185 (Pt-3):1984	Observed Value	Test Method
Length	600±5 mm	600	IS 2185 (Pt-3):1984
Height	200±5 mm	200	
Width	230±5 mm	225	
Oven Dry Density (Kg/m ³)	551–650	577	IS 6441 (Pt-1):1972
Compressive Strength (Avg. of 12 units, N/mm ²)	(Grade 1) 4.0 Min. (Grade 2) 3.0 Min.	4.4	IS 6441 (Pt-5):1972

Analysis of Projectile Impact Data

A sample of 12 specimens underwent testing within the indoor environment of the Ballistics Range. The firing was done at a fixed 5 m distance from the target, with an IR light gate positioned 2.5 m from the barrel’s muzzle end to measure initial projectile velocity (gate data transmitted to a computer via Ethernet, with velocity calculations conducted through BMS Test Velocity LG software). A laser light integrated into the firing setup facilitated precise targeting of the sample’s center. The firing setup is visually represented in Figure 2 for reference.

RESULTS

Firing and Impact Analysis

The firing process encompassed four angles: 0°, 15°, 30°, and 45°, achieved by adjusting the motorized moving table to the right. Each shot was directed at the center of the AAC block samples. In Study 03, identical AAC block samples were used for each angle of impact. Upon completion of each

test, samples were removed from the motorized table, and comprehensive photographs of entry and exit holes were captured. The ballistic impact of the fired 9 mm projectiles on AAC blocks was subsequently examined.

Visual examination was followed by precise measurements of different parameters, including entry and exit hole diameters, depth of penetration (in instances without exit holes), and depth of crater formation due to scabbing. Vernier calipers and scales facilitated measurements. Bullet weight and dimensions were also recorded. During analysis, damaged areas of the samples were photographed, and fracture patterns were observed. These patterns were affected by sample thickness, surface area, and bullet energy loss upon impact [2, 9].

Energy Analysis and Calculations

For energy analysis, the bullet mass was considered constant. The study employed the kinetic energy formula:

$$K.E. = \frac{1}{2}mv^2; \tag{1}$$

To determine impact energy, we used the following equation:

$$E = m \frac{(v_x^2 + v_y^2)}{2}, \tag{2}$$

$$v_x^2 = v \cos \theta ,$$

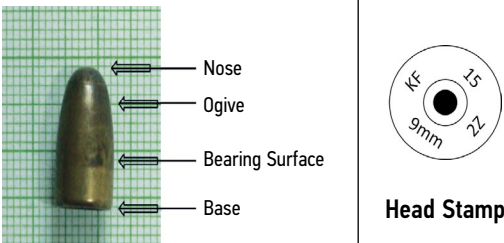
$$v_y^2 = v \sin \theta - gt ,$$

where

- *m* is the initial bullet mass in kg before surface impact
- *v* is the mean muzzle velocity in m/s determined using an IR gate 2.5 m from the barrel’s muzzle end
- *v_x²* and *v_y²* represent the horizontal and vertical velocity components, respectively, of the moving projectile (m/s)
- *θ* is the angle of impact in degrees
- *g* denotes the acceleration due to gravity (assumed as 9.8 m/s)
- *t* is the time of impact (considered as 0.01 s)

For impact energy calculations, mean muzzle velocity was considered. Entry and exit hole diameters were recorded using vernier calipers, and GraphPad Prism 9.3.1 was used for graph plotting. As entry holes were not perfect circles due

Table 2. Observed Standard Parameters of 9 mm Round Nose, FMJ Projectile

	
FMJ Round Nose Projectile (9 mm)	
Length	14.89 mm
Weight	7.507 g
Base Diameter (Caliber)	8.96 mm
Tip Diameter	7.37 mm
Neck Diameter	8.52 mm
Propellant Filling in Case	0.450 g (approx.)
Muzzle Velocity	430±15 m/s

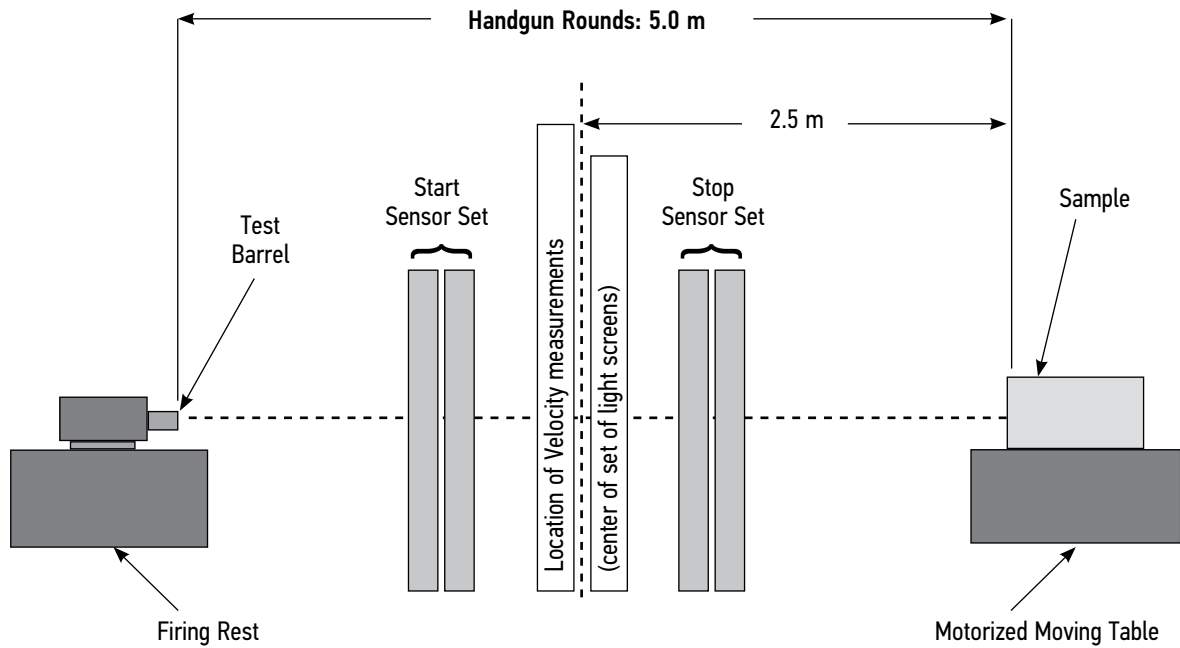


Fig. 2. Graphical Representation of Firing Test Setup.

to friction and point of impact variance on fly-ash blocks, the best-fit ellipse method [5, 10, 11, 12] was used to accurately determine impact angles. Recovered bullets underwent analysis for deformations by measuring length, weight, base, neck, and tip diameters and comparing them against standard 9 mm bullet parameters.

Impact Energy Analysis

Using equations 1 and 2, we can establish a relationship between the angle of impact and energy loss. The mass of the bullet was considered constant at the point of impact, despite potential deformations occurring during the impact but not before that. The results are summarized in Table 3.

From Table 3 and Figures 3 and 4 (created using GraphPad Prism 9.3.1), it is evident that increasing the angle of firing impact initially leads to heightened impact energy. Beyond a certain angle, however, there’s a noticeable decline in impact energy. The observed fluctuation in the curve might be attributed to reaching a critical angle where the curve transitions from a gradual increase to a steep decrease.

This critical angle signifies the angle of elevation at which the projectile starts to ricochet. The absence of penetration at a 45° angle could be attributed to the maximum energy loss at this angle. Conversely, the most substantial damage occurred at a 0° impact angle due to no energy loss as there is no vertical velocity component, resulting in a non-parabolic trajectory. In contrast, any angle other than this exhibits a parabolic trajectory with a vertical velocity component influenced by gravity’s acceleration (–g). The projectile’s horizontal velocity component remains constant across all firing angles.

Determination of Angle of Impact from Entry Hole and Fracture Patterns

Bullets penetrated all samples at all study angles, creating entry holes with no damage visible at 0° and 15°. At 30° and 45°, some spalling was evident near entry holes, as illustrated in Figure 5. On the reverse surface, the bullet perforated with fragmentation/flying debris, except at a 45°

Table 3. Energy Impact and Loss at the Site of Impact w.r.t. Angle of Impact

Angle of Impact	Initial Energy ⁱ (J) (A)	Impact Energy ⁱⁱ (J) (B)	Energy Loss ⁱⁱⁱ (J) (C=A-B)	% Loss of Energy ⁱⁱⁱ , $\left(\frac{C}{A} \times 100\right)$
0°	694.02	694.02	0.00	0%
15°		694.04	-0.02	-0.003%
30°		693.86	0.16	0.023%
45°		693.82	0.20	0.029%

Note: (i) — distance from the muzzle end (2.5m); (ii) — at point of impact; (iii) — loss in K.E of bullet at time t = 0.01s.

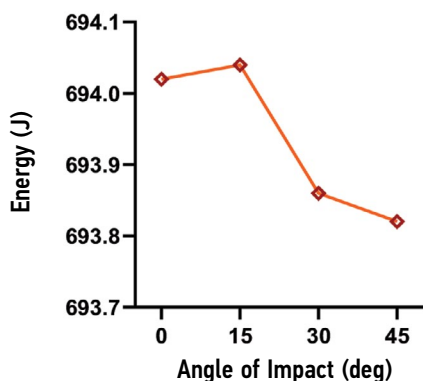


Fig. 3. Impact Energy.

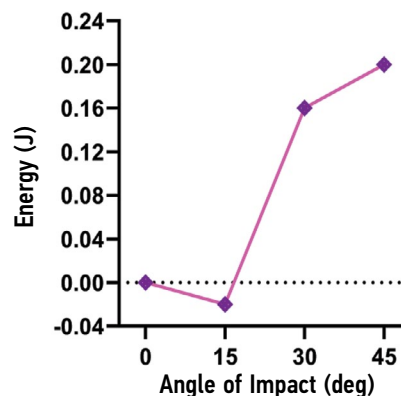


Fig. 4. Energy Loss.

impact angle, which showed no back damage/perforation (Figure 6). Table 4 depicts fracture patterns at entry and exit holes for different angles (0°, 15°, 30°, and 45°).

The mean diametric distances of entry and exit holes were measured and graphed (Table 5, Figure 7). Graphical analysis showed that the entry hole diameter increases with higher impact angles, attributed to a greater surface area of the bullet that comes in contact with the sample at the point of impact. Conversely, the exit hole diameter decreases with increasing angles. At 0°, the exit hole diameter is greater than that of the entry hole due to no energy loss at the point of impact, resulting in substantial damage. For other cases, the exit hole diameter progressively shrinks, with no perforation

observed at a 45° impact angle due to increased energy loss at the point of impact.

Crater depth measurements from the exit hole were 32.23 mm, 29 mm, and 19.90 mm for 0°, 15°, and 30° angles of impact, respectively. This shows that at 30°, the bullet traveled the farthest, causing the least damage due to the maximal energy loss upon impact, compared to 0° and 15°. Impact damage parameters of the major and minor axis (length, *l*, and width, *w*, of the elliptical shape of the entry hole) were measured and averaged (Table 6). The observed α and calculated θ values for the angle of impact indicated that the calculated angle provided an approximation for $90 - \alpha$ rather than α , which is the actual angle of impact. Therefore, to understand the deviation and error in the known

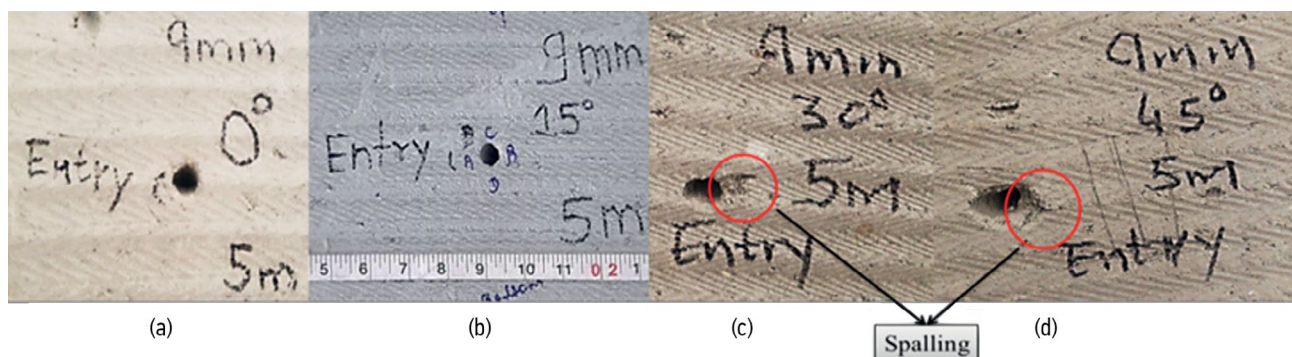


Fig. 5. Entry Holes at 5m Range at Different Angles — 0°, 15°, 30°, 45°, Respectively.

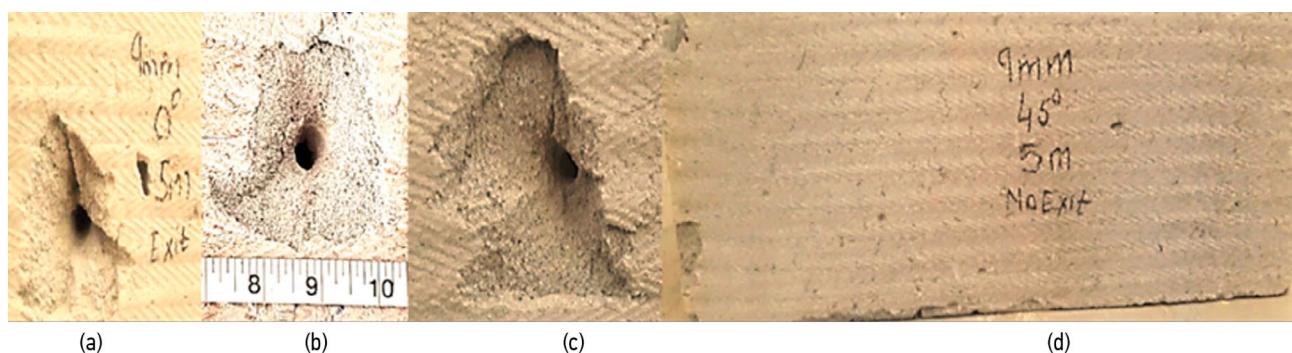


Fig. 6. Exit Holes at 5m Range at Different Angles: 0°, 15°, 30°, and 45°.

Table 4. Fracture Patterns Observed on AAC Blocks

Angle of Impact	Entry Damage	Exit Damage
0°	<ul style="list-style-type: none"> • Penetration • No loss in impact energy • Maximum bullet tip interaction with the target surface results in the minimum mean diameter for the entry hole 	<ul style="list-style-type: none"> • Perforation • Mean diameter of the exit hole is greater than the mean diameter of the entry hole and is maximum
15°	<ul style="list-style-type: none"> • Penetration • Negligible loss in impact energy • Decreased bullet tip interaction with the target surface compared to 0°, and the mean diameter for the entry hole lies close to that of 0° 	<ul style="list-style-type: none"> • Perforation • Mean diameter of the exit hole is lesser than the mean diameter of the entry hole and is lesser than that of 0°
30°	<ul style="list-style-type: none"> • Penetration and spalling • Visible loss in impact energy • Decreased bullet tip interaction with the target surface compared to 15°, and the mean diameter for the entry hole lies close to that of 15° 	<ul style="list-style-type: none"> • Perforation • Mean diameter of the exit hole is lesser than the mean diameter of the entry hole and lies close to that of 15°
45°	<ul style="list-style-type: none"> • Penetration and spalling • Maximum loss in impact energy • Minimum bullet tip interaction with the target surface results in the maximum mean diameter for the entry hole 	<ul style="list-style-type: none"> • No back damage/perforation • No exit hole was present

Table 5. Diameter of Entry and Exit Holes w.r.t. Angle of Impact

Angle of Impact	No. of Shots Fired	Mean Diameter of Entry Hole (mm)	Mean Diameter of Exit Hole (mm)
0°	3	13.67	24.93
15°	3	14.42	12.36
30°	3	14.26	12.09
45°	3	22.93	No Perforation

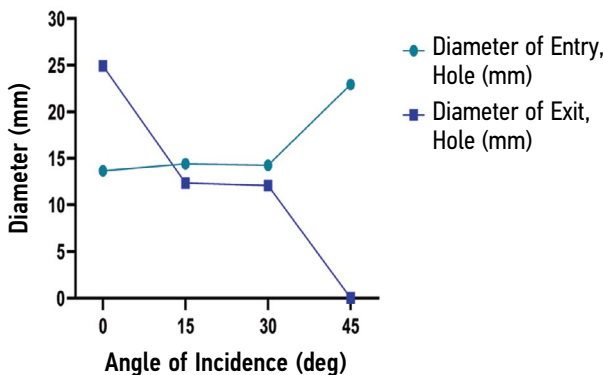


Fig. 7. Diameter of Entry Hole vs. Exit Hole.

and calculated angles, a correction was introduced in the formula:

$$\theta = \sin^{-1} \frac{w}{l} \times \frac{180}{\pi}, (3)$$

where, $\theta' = 90 - \left(\sin^{-1} \left(\frac{w}{l} \right) \times \frac{180}{\pi} \right)$.

Angle of Impact Error and Regression Analysis

On calculating the error between known and calculated values for the angle of impact, a non-uniform variation becomes evident, with the maximum variation observed at 30° and the minimum at 0°. However, it is interesting to note that the least error occurs at 30°, whereas the highest error occurs at 0°, indicating a deviation from expected behavior. Conversely, angles 15° and 45° show consistent patterns without such anomalies. Employing both linear and non-linear regression on the data and plotting the non-linear regression (Figure 8), it was determined that the absolute error pattern aligned best with a quadratic equation. Utilizing GraphPad Prism 9.3.1, a statistically significant result was achieved through the least-squares fit (R^2 value 0.9922).

Figure 9 shows the trajectory of the bullet upon impact, entering the fly-ash block and creating a small hole. This happened when fired from a 5m range at a 0° impact angle.

Physical Examination of the Recovered Bullets

Bullet recovery was achieved at a 30° impact angle, while at 45°, recovery required cutting the AAC block with a disc

Table 6. Calculated and Known Angle of Impact

	Tested parameters			
Angle of Impact (α)	0°	15°	30°	45°
No. of Shots Fired	3	3	3	3
Mean Major Axis (mm)	15.83	15.64	16.85	29.37
Mean Minor Axis (mm)	15.75	14.99	14.48	19.99
Calculated Angle of Impact $\theta = \sin^{-1}\left(\frac{w}{l}\right) \times \frac{180}{\pi}$	84.24°	73.42°	59.24°	43.01°
Calculated Angle of Impact with Corrected Formula ($\theta' = 90 - \theta$)	5.76°	16.58°	30.76°	46.99°
Error ($\theta' - \alpha$)	5.76°	1.58°	0.76°	1.99°
Standard Deviation	0.04	0.07	0.17	0.10

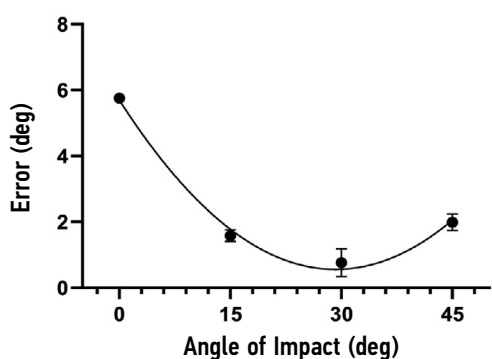


Fig. 8. Least Squares Fit.

grinder. The recovered bullets showed the right-hand rifling with a clockwise twist, characterized by one turn and six lands and grooves—indicative of a 9 × 19 mm test barrel. Deformation was observed at the tip without fragmentation.

Table 7 suggests that at a 30° impact angle, more pronounced variations in various recovered bullet parameters were noted compared to the 45° angle.

DISCUSSION

The study’s results indicated penetration and perforation fracture modes at impact angles of 0°, 15°, and 30° while spalling occurred at 30° and 45° angles. No perforations were found at 45°, causing no damage to the AAC blocks’ backside. Notably, a similar study on steel fiber-reinforced concrete panels with varying thicknesses and fiber content reported consistent fracture patterns upon impact with a 9mm FMJ bullet at the center, indicating that damage was not observed beyond 40 mm [1]. These panels displayed excellent impact resistance due to their thickness and steel fiber content. However, in our study, the surface area of

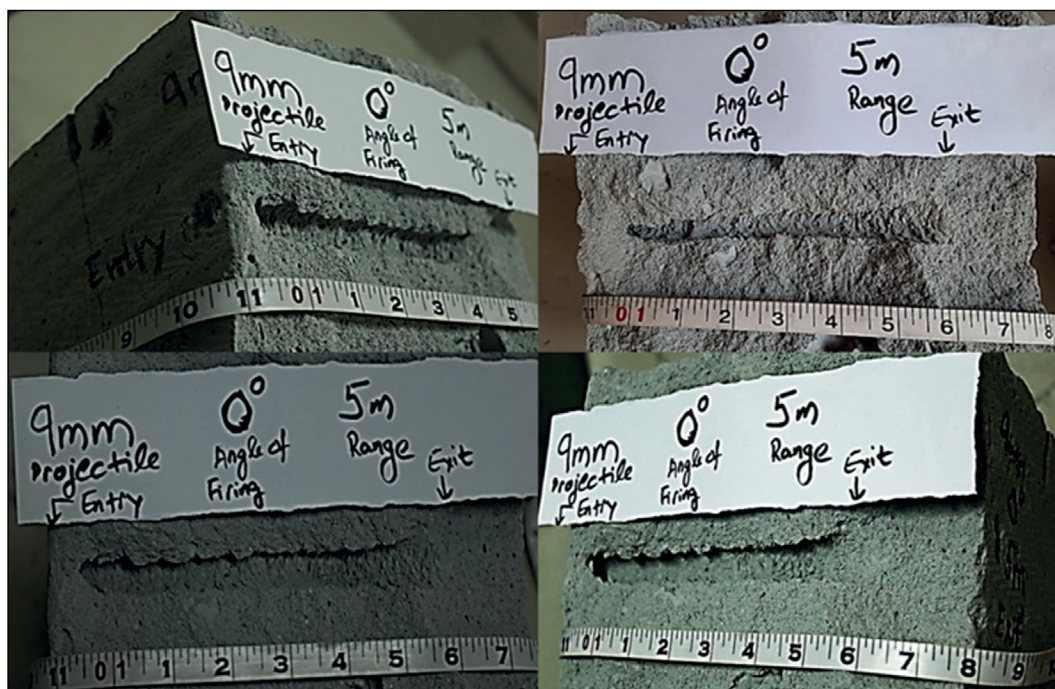


Fig. 9. Trajectory of the Impacted Bullet Fired at 0° from 5m Range.

Table 7. Analysis of the Recovered Bullets w.r.t. Angle of Impact

Angle of Impact	No. of Shots Fired	No. of Bullets Recovered	Dimensions of Bullet		Difference in Dimensions Before and After Firing (C = A-B)	% Loss in Dimensions ($\frac{C}{A} \times 100$)
			Standard (A)	After Firing (B)		
Length						
30°	3	1	14.89 mm	14.02 mm	0.87 mm	5.84%
45°	3	1		14.51 mm	0.38 mm	2.55%
Weight						
30°	3	1	7.507 g	7.430 g	0.077 g	1.03%
45°	3	1		7.445 g	0.062 g	0.83%
Base Diameter (Caliber)						
30°	3	1	8.96 mm	8.86 mm	0.10 mm	1.12%
45°	3	1		8.95 mm	0.01 mm	0.11%
Ogive Diameter						
30°	3	1	8.52 mm	8.87 mm	0.35 mm	4.11%
45°	3	1		8.66 mm	0.14 mm	1.64%
Tip Diameter						
30°	3	1	7.37 mm	6.83 mm	0.54 mm	7.33%
45°	3	1		7.20 mm	0.17 mm	2.31%

the bullet and the contact time between the bullet tip and the target surface emerged as influential factors in fracture patterns. Another study suggested that variations in fracture modes across different angles can be attributed to concrete sample composition, with energy absorption partially converting to fracture energy, thereby generating fracture surfaces [4]. This energy absorption trend was consistent with a study involving steel fiber-reinforced concrete panels, where impact energy absorption increased with greater thickness and fiber content [1].

Our analysis focused on bullet impact energy to understand the diverse fracture modes at different impact angles. Maximum damage and fragmentation were observed at 0°, associated with minimal energy loss. Conversely, at 45°, the projectile experienced significant energy loss, causing it to stop within the target without perforation. The impact energy analysis of the 9mm FMJ projectile on the target surface, fired from a 5m range, hinted at a possible critical angle attainment between 15° and 30°. A review study explored parameters for reconstructing crime scenes involving inanimate objects, highlighting distinct impact marks on different target surfaces. Concrete and wooden surfaces with round or elliptical entry holes and the ejection of surface materials from exit holes indicated the non-yielding behavior of these materials [12]. In our study, the measured entry hole diameters exceeded the caliber of the 9mm projectile, suggesting the non-yielding behavior of AAC blocks. It is interesting to know that a deviation was observed between the angle of impact calculated using the best-fit ellipse method and that observed on AAC blocks.

Different studies utilizing best-fit ellipse and 2D ellipse methods were conducted to accurately determine the angle of impact and the repeatability of single bullet impacts. While the ellipse method effectively calculated impact angles up to 30°, an increase in impact angle tended to make impact sizes more circular than elliptical. This observation aligned with a previous study where circular impacts at 0° angle of impact exhibited reduced accuracy [10, 11]. Physical examination of the recovered bullets revealed characteristics of deformation without fragmentation. Additionally, AAC block components and rifling details were on the bullets, providing potential evidence for linking the bullets to gunshot holes and firearms at crime scenes.

CONCLUSION

Bullet recovery from crime scenes holds substantial evidential value aiding in determining firearm characteristics, caliber, and projectile features such as the number of lands and grooves. Furthermore, microscopic examination and characterization help in identifying the weapon type, facilitating bullet-weapon linkage. Our study focused on understanding the angular firing impact of a 9 mm round nose full metal jacketed projectile on AAC blocks. A noticeable trend was observed between the angle of impact and the entry and exit hole diameters. Greater impact angles led to larger entry hole diameters and smaller exit hole diameters, attributable to impact energy and bullet-surface contact area at the point of impact. At 0°, the bullet tip interaction with the target surface was maximized, causing significant

impact at the exit point. The deviation in calculating the angle of impact using the best-fit ellipse method was addressed by modification, yielding a non-homogenous variation best explained by a quadratic equation plot. A similar study focused on the trajectory simulation of 7.62 mm/.308" rifle bullets was previously conducted by one of the authors using numerical solutions of point-mass equations of motion [13].

Research Limitations

This pilot study's limitations include its single impact on a single AAC block, with bullets not being recovered for 0° and 15° impact angles, preventing inferential analysis. For a more comprehensive analysis and crime scene reconstruction, studying a wall with multiple bullet impacts could be beneficial. Future research could delve into penetration, ricochet, and trajectory simulation, exploring combinations of ammunition and AAC blocks commonly used in criminal activities.

ADDITIONAL INFORMATION

Funding source. This study was not supported by any external sources of funding.

Competing interests. The authors declare that they have no competing interests.

REFERENCES

1. Heard B. Handbook of firearms and ballistics, 2nd ed. Hoboken, N.J.: Wiley; 2013.
2. Jamnam S, Maho B, Techaphatthanakon A, et al. Steel fiber reinforced concrete panels subjected to impact projectiles with different caliber sizes and muzzle energies. *Case Studies Construction Materials*. 2020;(13):e0030. doi: 10.1016/j.cscm.2020.e00360
3. Backman M. Terminal ballistics. China Lake, Calif: Naval Weapons Center; 1976. 232 p.
4. Werner S, Thienel K, Kustermann A. Study of fractured surfaces of concrete caused by projectile impact. *Int J Impact Engineering*. 2013;(52):23–27. doi: 10.1016/j.ijimpeng.2012.09.005
5. Mattijssen E, Kerkhoff W. Bullet trajectory reconstruction: Methods, accuracy and precision. *Forensic Sci Int*. 2016;(262):204–211. doi: 10.1016/j.forsciint.2016.03.039
6. Bureau of Indian Standards: E-Sale Search Result. Standardsbis. bsbedge.com; 1984. [Online]. Available from: https://standardsbis.bsbedge.com/BIS_SearchStandard.aspx?keyword=autoclaved%20&id=0. Accessed: 11 Feb 2022.
7. AAC Block. Satyambuildtech.com. [Online]. Available from: <https://www.satyambuildtech.com>. Accessed: 28 Apr 2022.
8. Visit of Bimstec Nations Army Chiefs, Ficci.in, 2018. [Online]. Available from: https://ficci.in/events/23972/ISP/FICCI_ADB_Defence_EquipmentCatalogue_For_BIMSTEC_Nations.pdf. Accessed: 13 May 2022.
9. Li Q, Chen X. Penetration and perforation into metallic targets by a non-deformable projectile. *Engineering Plasticity Impact Dynamics*. 2001. doi: 10.1142/9789812794536_0010
10. Liscio E, Imran R. Angle of impact determination from bullet holes in a metal surface. *Forensic Sci Int*. 2020;(317):110504. doi: 10.1016/j.forsciint.2020.110504
11. Walters M, Liscio E. The accuracy and repeatability of reconstructing single bullet impacts using the 2D ellipse method. *J Forensic Sci*. 2020;65(4):1120–1127. doi: 10.1111/1556-4029.14309
12. Nordin F, Bominathan U, Abdullah A, Chang K. Forensic significance of gunshot impact marks on inanimate objects: The need for translational research. *J Forensic Sci*. 2019;65(1):11–25. doi: 10.1111/1556-4029
13. Gangopadhyay S, Rohatgi R. Trajectory simulations by the numerical solution of the point-mass equations of motion for 7.62 mm/.308" rifle bullets. *Russ J Forensic Med*. 2022;8(2):23–36. (In Russ). doi: 10.17816/fm730

СПИСОК ЛИТЕРАТУРЫ

1. Heard B. Handbook of firearms and ballistics, 2nd ed. Hoboken, N.J.: Wiley, 2013.
2. Jamnam S., Maho B., Techaphatthanakon A., et al. Steel fiber reinforced concrete panels subjected to impact projectiles with different caliber sizes and muzzle energies // *Case Studies Construction Materials*. 2020. N 13. P. e0030.
3. Backman M. Terminal ballistics. China Lake, Calif: Naval Weapons Center, 1976. 232 p.

4. Werner S., Thienel K., Kustermann A. Study of fractured surfaces of concrete caused by projectile impact // *Int J Impact Engineering*. 2013. N 52. P. 23–27.
5. Mattijssen E., Kerkhoff W. Bullet trajectory reconstruction: Methods, accuracy and precision // *Forensic Sci Int*. 2016. N 262. P. 204–211.
6. Bureau of Indian Standards: E-Sale Search Result. Standardsbis.bsbedge.com, 1984. [интернет-ресурс]. Режим доступа: https://standardsbis.bsbedge.com/BIS_SearchStandard.aspx?keyword=autoclaved%20&id=0. Дата обращения: 11.02.2022.
7. AAC Block. Satyambuildtech.com. [интернет-ресурс]. Режим доступа: <https://www.satyambuildtech.com>. Дата обращения: 28.04.2022.
8. Visit of Bimstec Nations Army Chiefs, Ficci.in, 2018. [интернет-ресурс]. Режим доступа: https://ficci.in/events/23972/ISP/FICCI_ADB_Defence_EquipmentCatalogue_For_BIMSTEC_Nations.pdf. Дата обращения: 13.05.2022.
9. Li Q., Chen X. Penetration and perforation into metallic targets by a non-deformable projectile // *Engineering Plasticity Impact Dynamics*. 2001.
10. Liscio E., Imran R. Angle of impact determination from bullet holes in a metal surface // *Forensic Sci Int*. 2020. N 317. P. 110504.
11. Walters M., Liscio E. The accuracy and repeatability of reconstructing single bullet impacts using the 2D ellipse method // *J Forensic Sci*. 2020. Vol. 65, N 4. P. 1120–1127.
12. Nordin F., Bominathan U., Abdullah A., Chang K. Forensic significance of gunshot impact marks on inanimate objects: The need for translational research // *J Forensic Sci*. 2019. Vol. 65, N 1, P. 11–25.
13. Gangopadhyay S., Rohatgi R. Trajectory simulations by the numerical solution of the point-mass equations of motion for 7.62 mm/.308" rifle bullets // *Russ J Forensic Med*. 2022. Vol. 8, N 2. P. 23–36. doi: 10.17816/fm730

AUTHORS' INFO

* **Dr. Richa Rohatgi**, MD, Dr. Sci. (Med.), Assistant Professor, Forensic Science;
address: New Delhi, 110085, India;
ORCID: 0000-0001-5514-953X;
e-mail: rrohatgi2020@gmail.com

Malika Singh, MSc Forensic Science;
ORCID: 0009-0005-4749-1622;
e-mail: singhmalika98@gmail.com

Saurabh Kumar, MD, Dr. Sci. (Med.);
ORCID: 0000-0001-8442-1096;
e-mail: saurabh.kumar@nfsu.ac.in

Sanjay Gupta, MD, Dr. Sci. (Med.), Professor;
ORCID: 0000-0003-3829-3155;
e-mail: drsanjaymdfm@gmail.com

ОБ АВТОРАХ

* **Рича Рохатги**, д-р мед. наук, доцент;
адрес: Нью-Дели, 110085, Индия;
ORCID: 0000-0001-5514-953X;
e-mail: rrohatgi2020@gmail.com

Малика Сингх;
ORCID: 0009-0005-4749-1622;
e-mail: singhmalika98@gmail.com

Саураб Кумар, д-р мед. наук;
ORCID: 0000-0001-8442-1096;
e-mail: saurabh.kumar@nfsu.ac.in

Санджай Гупта, д-р мед. наук, профессор;
ORCID: 0000-0003-3829-3155;
e-mail: drsanjaymdfm@gmail.com

* Corresponding author / Автор, ответственный за переписку